2023

# A High-Pressure Shock Tube Study of Hydrogen and Ammonia Addition to Natural Gas for Reduced Carbon Emissions in Power Generation Gas Turbines

Michael Pierro
*University of Central Florida*

# A HIGH-PRESSURE SHOCK TUBE STUDY OF HYDROGEN AND AMMONIA ADDITION TO NATURAL GAS FOR REDUCED CARBON EMISSIONS IN POWER GENERATION GAS TURBINES

by

MICHAEL PIERRO
B.S. University of Central Florida, 2020

A thesis submitted in partial fulfillment of the requirements
for the degree of Master of Science
in the Department of Mechanical and Aerospace Engineering
in the College of Engineering and Computer Science
at the University of Central Florida
Orlando, Florida

Summer Term
2023

Major Professor: Subith S. Vasu

# ABSTRACT

Ignition delay times from undiluted mixtures of natural gas (NG)/$H_2$/Air and NG/$NH_3$/Air were measured using a high-pressure shock tube at the University of Central Florida. The combustion temperatures were experimentally tested between 1000-1500 K near a constant pressure of 25 bar. Mixtures were kept undiluted to replicate the same chemistry pathways seen in gas turbine combustion chambers. Recorded combustion pressures exceeded 200 bar due to the large energy release, hence why these were performed at the high-pressure shock tube facility. The data is compared to the predictions of the NUIGMech 1.1 mechanism for chemical kinetic model validation and refinement. An exceptional agreement was shown for stoichiometric conditions in all cases but strayed at lean and rich equivalence ratios, especially in the lower temperature regime of $H_2$ addition and all temperature ranges of the baseline NG mixture. Hydrogen addition also decreased ignition delay times by nearly 90%, while $NH_3$ fuel addition made no noticeable difference in ignition delay time. NG/$NH_3$ exhibited similar chemistry to pure NG under the same conditions, which is shown in a sensitivity analysis, demonstrating hydrogen chemistry to be dominant in NG/$H_2$ mixtures and hydrocarbon chemistry to be dominant in NG/$NH_3$ mixtures. The reaction $CH_3 + O_2 = CH_3O + O$ is identified and suggested as a possible modification target to improve model performance. Increasing the robustness of chemical kinetic models via experimental validation will directly aid in designing next-generation combustion chambers for use in gas turbines, which in turn will greatly lower global emissions and reduce greenhouse effects.

*to Mom, Dad, and Megan Pierro*

# ACKNOWLEDGMENTS

I would first like to thank my advisor, Prof. Subith Vasu, for his guidance and support as I start the journey into my research career. I am forever grateful to him for allowing me to pursue my interest in combustion and having confidence in me to perform to the best of my abilities. I want to acknowledge my parents, Don and Kerry Pierro, for their love and support during all of the years I have spent away from home and making me the person I am today. I also want to specially thank my lab mentors, Dr. Justin Urso for his expertise in just about everything to our Formula 1 conversations, Dr. Cory Kinney for his incredible Python and fundamental knowledge to our great chess matches, and Dr. Andrew Laich for his combustion and laser knowledge to our automotive talks, but most of all, for all being so willing to teach, advise, and befriend me. I could not have asked for better peers to be with and cherished all of my time spent with you all. This goes to all the other former and current members of OTC as well, in particular, JP McGaunn, Chris Dennis, and Marley Albright, for whom I have been with from the start. Lastly, I want to thank my committee members, Dr. Anthony Terracciano and Dr. Sagnik Mazumdar, for taking the time to be part of my thesis committee.

The material in this work was supported by the Department of Energy (DE-FE0032072), the NASA Florida Space Grant Consortium, and the University of Central Florida (UCF). Feedback from Mitsubishi Power and General Electric is also acknowledged.

# TABLE OF CONTENTS

# LIST OF FIGURES

# LIST OF TABLES

# CHAPTER 1: INTRODUCTION

For the past century, fossil fuel combustion has driven the global economy and led the energy sector as the main electricity provider. Although natural gas (NG) has replaced coal as a cleaner burning fuel, carbon dioxide ($CO_2$) is still a main product of combustion. As part of the worldwide initiative to decrease carbon emissions, studies into hydrogen ($H_2$) and ammonia ($NH_3$) combustion for uses in gas turbines have accelerated. Both $H_2$ and $NH_3$ are favorable as NG replacements due to their carbon-free emissions; however, both entail major challenges. The storage, transportation, and flame stability of these fuel alternatives has yet to be properly controlled. There are also concerns about the tangibility of these fuels as they both require methane steam reforming to be produced, but Haugen *et al*. have shown methods of capturing the $CO_2$ produced during the reforming process [1].

Hydrogen is a favorable fuel because it does not produce carbon nor fuel-nitrogen oxide ($NO_x$) emissions (unlike ammonia) when burned with pure oxygen ($O_2$) but draws major issues with its storage, transportation, and high reactivity. $H_2$ is also prone to flame flashback because of its high burning velocity [2, 3], which causes the flame to propagate upstream of the designed location in the combustor. Conversely, blowout is a common issue encountered with $NH_3$ flame stability due to its slower chemical reactions [4, 5], where $NO_x$ emission levels are optimally low. When combusted, L-$NH_3$ has a higher volumetric energy density than L-$H_2$, but any ammonia combustor must also be able to confidently have near-complete combustion to prevent leftover toxic $NH_3$ molecules in the exhaust, or “ammonia slip”. On top of that, nitrous oxide ($N_2O$), another product from $NH_3$ combustion, has been said to potentially have a much larger impact on the climate than $CO_2$ itself [6] but can be effectively mitigated to some extent using selective

catalytic reduction (SCR) [7]. Ammonia can, however, be utilized to act as a hydrogen carrier. Through the reverse Haber-Bosch process, a heated catalytic surface (most likely ruthenium or iron) can be used to break up $2NH_3 \Leftrightarrow N_2 + 3H_2$ [8]. Additionally, there are already existing L-$NH_3$ pipelines that have proven reliable for decades and could be used for ammonia transportation [9, 10].

The combustion instabilities can be offset when premixed blends of NG/$NH_3$ or NG/$H_2$ are utilized, providing a stable and efficient flame with lowered carbonous and nitrogenous emissions while making minimal modifications to existing NG turbines [11, 12]. While flame speeds and emissions are more optimal using blends solely of $H_2$/$NH_3$, the infrastructure required to swap existing NG pipelines and turbomachinery would be an immensely expensive and time-consuming operation. Several studies have been performed to measure the combustion characteristics of these blends to find an optimum equivalence and fuel ratio during turbine operation, as outlined by Chai *et al*. [13]. By use of a robust chemical kinetic model, these fuel blends can be optimized using computational fluid dynamics (CFD) rather than experimental data. The scope of this project aims to experimentally study the ignition delay times (IDTs) of undiluted NG/$NH_3$/Air and NG/$H_2$/Air mixtures at the relevant pressures and temperatures (25 bar, 1000-1500 K) in order to validate and refine the current chemical kinetic mechanisms.

# CHAPTER 2: LITERATURE REVIEW

While much work has been performed over the past decade to study NG/$H_2$ mixtures, and few recent studies have looked into NG/$NH_3$ blends, little have tested undiluted mixtures at the temperatures and pressures experienced in gas turbine combustors. Previous ignition delay time measurements of $H_2$ addition into methane ($CH_4$) at elevated pressures by Gersen *et al*. demonstrated that mixtures containing less than 20% $H_2$ had a modest effect on ignition whereas 50% addition dramatically decreased IDT [14]. More shock tube studies by Herzler and Naumann and Huang *et al*. both found that chemical kinetic model performance decreased with increasing addition of $H_2$ [15, 16]. De Vries and Petersen [17] studied undiluted lean ($\Phi$=0.5) mixtures of pure NG/$H_2$ mixtures near the same conditions presented in the current study and found weak ignition to be prevalent. Weak ignition, in comparison to strong ignition, is a common issue with high-fuel-containing mixtures in the shock tube. As noted by De Vries and Petersen [17], there must be a distinction made between these two ignition events to properly build a chemical kinetic model. Similar work done by Laich *et al*. [18] also showed non-idealities for high-fuel-loaded mixtures of methane at lower temperatures near 15 bar.

Shock tube studies of methane addition into ammonia near 40 bar by Shu *et al*. revealed that increasing methane concentrations increased reactivity but conversely increased both CO and NO emissions [19]. Work by Baker *et al*. [20] has also already been performed at lower pressures and higher temperatures using diluted mixtures as an initiative to develop a robust NG/$H_2$/$NH_3$ model entitled UCF 2022. Similarly, mechanism development and reduction by Li *et al*. specifically targeted $CH_4$/$H_2$/$NH_3$ mixtures however does not encompass alkanes larger than $C_2$

[21]. This paper seeks to extend the pressure range of the chemical kinetic models as well as validate the ignition properties for undiluted mixtures of $H_2$ and $NH_3$ addition to NG.

# CHAPTER 3: EXPERIMENTAL METHODS

## 3.1 Shock Tubes

Mixtures were shock-heated and auto-ignited using a high-pressure shock tube at the University of Central Florida's (UCF) High-Pressure Extended Range Shock Tube for Advanced Research (HiPER-STAR) facility [22]. A shock tube allows for consistent replication of combustion studies through velocity control of the generated shock. The tube is separated into two sections. The high-pressure section (referred to as the driver) is filled with a non-reactive gas, in this case, a tailored mixture of ultra-high purity (Nexair, 99.999%) helium (He) and ultra-high purity (Nexair, 99.999%) nitrogen ($N_2$) until the pre-scored aluminum diaphragm between the two sections is ruptured at the pre-determined break pressure. The large pressure difference following the diaphragm rupture forms a shock wave, which travels downstream of the shock tube. It should be noted that the driver gas tailoring is not used to extend test time (as commonly referred to in shock tube literature) but instead to target specific experimental pressure and temperature. The low-pressure section of the shock tube is referred to as the driven section, which contains the mixture of study and is heated initially by the incident shock wave, and then once again after the shock wave reflects off the end wall of the shock tube. The secondary heating from the reflected shock wave brings the volume behind the shock to the desired temperature and pressure of the study at stagnant conditions. Temperature and pressure measurements were calculated from an in-house Python ideal and real gas 1-D frozen shock equation solver (PyRGFROSH) [23] using the shock velocity from the time intervals between five piezoelectric sidewall dynamic pressure transducers downstream of the shock tube (shown in Figure 1). For the current study, the ideal gas solver was used. These were then validated by the State 5 pressure recording.

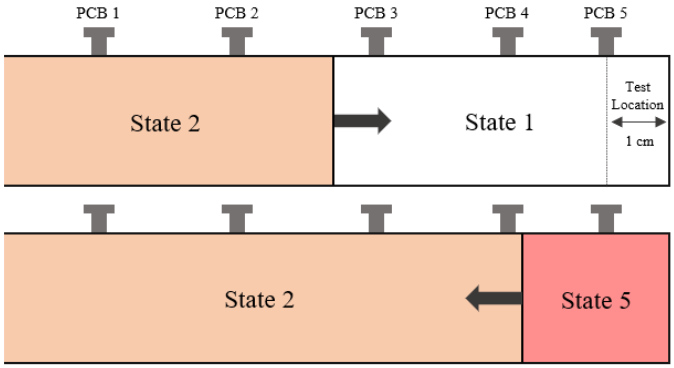


Figure 1:Visual representation of shock wave propagating downstream of the shock tube with pressure transducers in their approximate locations. Subscript 1 refers to the state properties before the arrival of the incident shock wave. State 5 is the test conditions after the reflected shock wave.

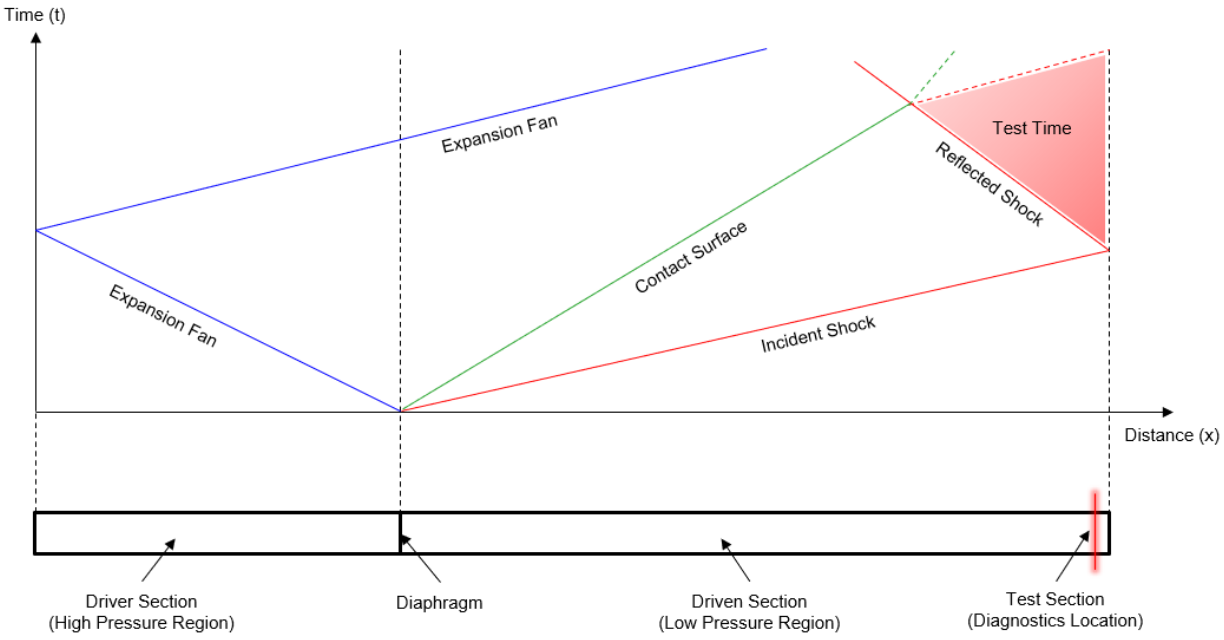


Figure 2: Distance-time (x-t) diagram of the shock tube, demonstrating the movement of shock waves during an experiment

## 3.2 Mixture Preparation

Mixtures were made using the partial pressures (assuming Dalton's law) calculated from mole fractions of balanced chemical equations and then pre-mixed in a magnetically stirred high-pressure mixing tank. As noted earlier, the mixtures were undiluted to replicate the chemistry during realistic gas turbine conditions, meaning the only gas constituents were fuel and synthetically made air. In all cases, the $O_2$:$N_2$ ratio was kept constant at 1:3.76. The NG mixture was a pre-made blend of 97.37614% $CH_4$, 2.25% $C_2H_6$, 0.077% $C_3H_8$, 0.00506% $C_4H_{10}$, 0.242% $N_2$, and 0.0498% $CO_2$, which was primary standard certified by Nexair. It is important to note that larger quantities of higher-order hydrocarbons can accelerate the ignition process and change reaction pathways therefore, lower concentrations of these were used in the study as an analog to industrial applications [24, 25]. Ultra-high purity (99.999%) $O_2$ and $N_2$ were also supplied by Nexair. A list of the mixture constituents is formatted below in Table 1. Hereafter, mixtures will be referred to by their designated names from the table. $NH_3$ is also known to adsorb into the stainless-steel shock tube [26], which could disrupt the purity of the mixture; however, when high molar concentrations of $NH_3$ are used, it has been experimentally determined by Pochet et al. that any adsorbed ppm quantities are not enough to have an effect on IDT [27]. Furthermore, the facility mixing tank is Teflon coated to further reduce this phenomenon.

Table 1: Fuel fraction of tested mixtures

| | NG | $H_2$ | $NH_3$ | Equivalence ratio (Φ) |
|---|---|---|---|---|
| Mix 1 | 1 | 0 | 0 | 1.0 |
| Mix 2 | 0.5 | 0.5 | 0 | 1.0 |
| Mix 3 | 0.5 | 0 | 0.5 | 1.0 |
| Mix 4 | 1 | 0 | 0 | 0.5 |
| Mix 5 | 0.5 | 0.5 | 0 | 0.5 |
| Mix 6 | 0.5 | 0 | 0.5 | 0.5 |
| Mix 7 | 1 | 0 | 0 | 2.0 |
| Mix 8 | 0.5 | 0.5 | 0 | 2.0 |
| Mix 9 | 0.5 | 0 | 0.5 | 2.0 |

### 3.3 IDT Measurements

All measurement devices are located at the test section of the shock tube, which is located 1 cm in front of the driven section endwall. Ports containing sapphire windows are used to allow optical access. Strong ignition IDTs ($\tau_{ign}$) were determined by the max peak in OH* chemiluminescence, starting from the point of max pressure rise in PCB 5 from the reflected shock wave (defined as "time-zero"), as shown in Figure 3. It should be noted that a secondary peak in the OH* trace is seen to be higher than the reported $\tau_{ign}$ in the case of Figure 3, which was present in a few ignition traces. This peak is not considered to be the "max peak" due to it coalescing with a post-detonation oscillation in the pressure trace. In all experiments, the OH* detector is radially located 180° from PCB 5, hence why oscillations in both traces are generally in phase with each

other. The post-detonation environments in undiluted mixtures are very dynamic and can create oscillations in the diagnostics, such as these.

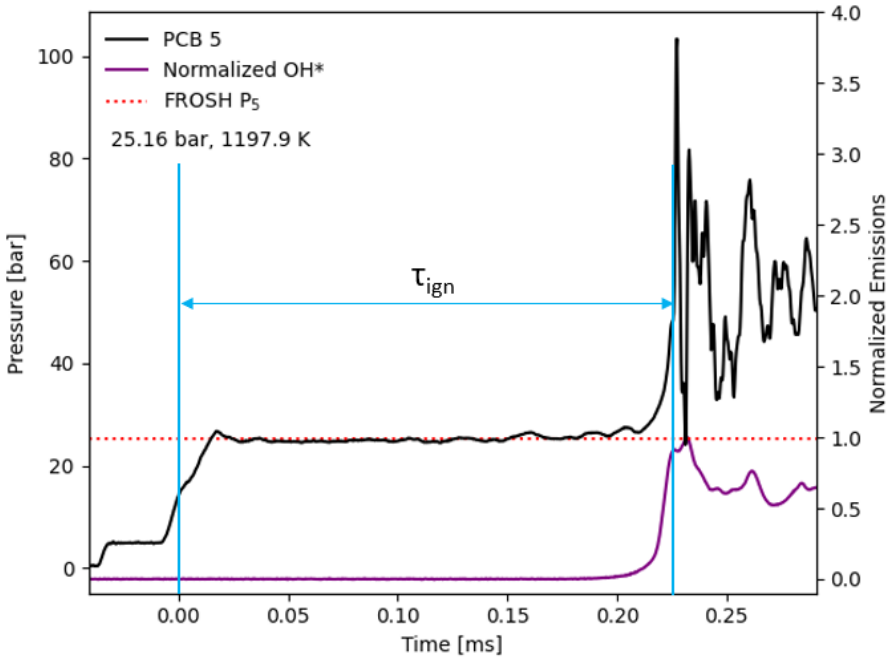


Figure 3: Homogenous pressure trace from Mix 2 using OH* max species concentration for determination of IDT.

The reasoning for calculating time-zero at the max pressure rise in PCB 5 from the reflected shock wave is that a bifurcated shock wave can be observed in the pressure signal due to measurements collected from sidewall-mounted transducers as opposed to endwall-mounted. Although the pressure nearest the wall is measuring the pressure caused by the boundary layer, it is assumed the core flow of the reflected shock wave is at the State 5 conditions, which is validated once the signal equilibrates several microseconds afterward. This concept is fully explained in detail by Petersen and Hanson [28]. Non-homogenous IDTs were not reported in this study due to uncertainty in the IDT determination, which was observed to be mixture independent in the lower temperature region, as discussed in Chapter 3.5.

As reported by Petersen [29], reporting IDTs from sidewall-mounted diagnostics for undiluted shock tube mixtures will make them slightly faster than endwall-based diagnostics due to strong ignition events volumetrically igniting the entire test section region. In these cases, the discrepancy comes from the time-zero measurement since the reflected shock wave arrives at the sidewall several microseconds after it departs from the endwall. In dilute mixtures cases, this phenomenon is not seen since strong ignition events generally do not occur, hence, sidewall-mounted diagnostics are not artificially faster because the ignition originates from the endwall rather than volumetric test section ignition. This reporting difference is considered to be both mixture and facility dependent. As said by Shu *et al*. [30], pure ammonia is slow to react and therefore strong ignition events are not seen. In addition, some facilities collect sidewall IDTs at different axial locations, affecting the time reporting difference when volumetric test section ignition occurs. In the case of this study, the shock tube was not capable of collecting endwall IDTs and therefore the variable endwall location was set to be 1 cm from the sidewall diagnostics to collect as close to the endwall as possible and reduce the time difference between endwall reported IDTs for strong ignition events. The time-zero difference was extrapolated using the reflected shock wave velocity from PyRGFROSH and calculated for each experiment to be between 25-27 μs, artificially making IDTs faster by this amount if volumetric ignition occurs in the test section region. For IDTs reported above 170 μs, this difference is within the uncertainty range however for higher temperature points with IDTs below this value, the uncertainty is increased to 16-38%.

## 3.4 Reaction Mechanism

Primarily a hydrocarbon-based chemical kinetic model, the NUIGMech 1.1 [31] contains 2845 species and 11260 reactions with alkanes up to $C_7$. The model encompasses all of the species used for the NG mixture in this study (up to $C_4$) while also containing an NO sub mechanism by Glarborg *et al*. [32] for $NH_3$ chemistry. Comparisons to the mechanism were made by applying the State 5 conditions to a constant volume 0-D batch reactor and simulated using a Cantera [33] Python code using the same IDT determination method as in the experimental calculations.

Following the experimental data is a sensitivity analysis of selected temperature points and mixtures performed in ANSYS CHEMKIN PRO 2022 R2 software [34]. Each sensitivity analysis was taken during the time at which the fuel was half consumed. In the case of blended mixtures, the slowest reacting of the two fuels was used in order to fully capture the synergistic chemistry. For the NG mixtures, the decomposition of $CH_4$ was used. A sensitivity analysis can help determine which chain reactions are prominent in the ignition sequence. When the sensitive reactions are compared across different temperature points and mixtures, conclusions about key chemistry differences can be inferred. In the case of this study, a sensitivity analysis is used to compare chemistry $H_2$ and $NH_3$ addition to baseline NG. The ANSYS CHEMKIN PRO sensitivity coefficients ($S$) are calculated using the methodology described by Neupane *et al*. [35],

$$S = \left(\frac{dX(t)}{dk_i}\right)\left(\frac{k_i}{X(t)}\right) \quad (1)$$

where $X$ is the species mole fraction over time and $k_i$ is the $i^{th}$ reaction rate. $S$ is then normalized ($S_N$) to the maximum sensitivity ($S_{max}$) of all sensitive reactions to the mixture using,

$$S_N = \frac{S_i}{S_{max}} \quad (2)$$

## 3.5 Pre-ignition Phenomenon

A common gas dynamic phenomenon experienced in shock tubes is a boundary layer forming while the reflected shock passes through the State 2 conditions. The boundary layer causes the reflected shock to bifurcate and form two oblique shocks on the leading and -trailing edges nearest the walls. Fundamental research by Mark [36] and Hollyer [37] found that the bifurcation is directly dependent on the specific heat ratio ($\gamma$) of the gaseous mixture. Monatomic gases, typically used in diluted shock tube mixtures, do not exhibit a boundary layer large enough to affect the shock wave because of their larger $\gamma$. However, diatomic and polyatomic mixtures, which have lower $\gamma$ values, bifurcate the shock wave and create a turbulent boundary layer. Yamashita *et al*. [38] performed advanced shock tube CFD and showed the triple point at which the oblique shocks meet the normal shock to be hotter than the core flow. The hot triple point then caused "hot spots" in the turbulent boundary layer, which are small pockets of high-temperature differences, as much as 50 K more for an 850 K State 5 temperature. The bifurcation also grows as the shock travels further, increasing the size of the localized hot spot in the triple point. Due to the low activation energy of the high-fuel mixture, the hot spot could locally ignite that region before the core flow. This is a non-ideal pre-ignition phenomenon that onsets the rest of the ignition, thus the mixture is not igniting at the theoretical post-shock temperature ($T_5$).

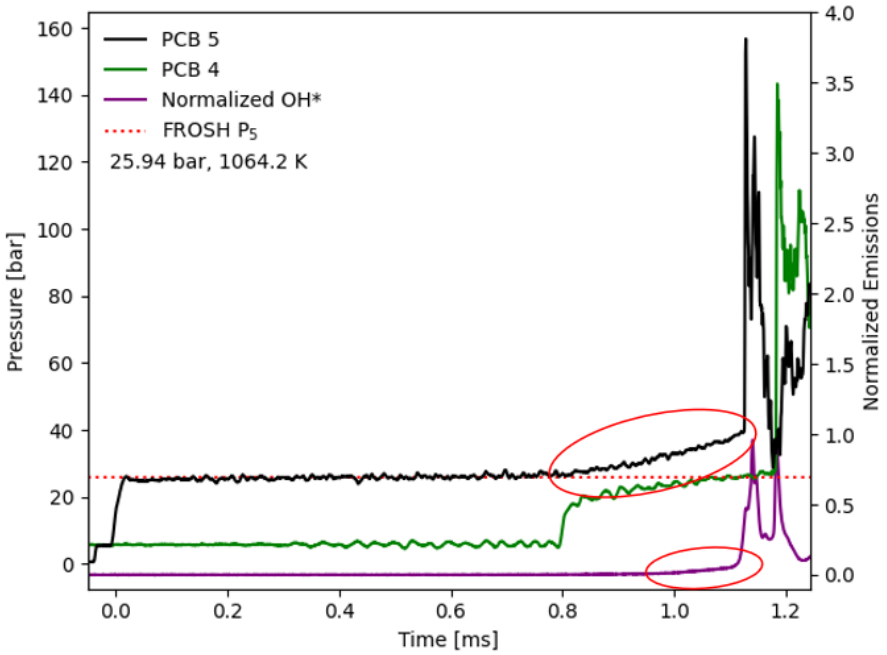


Figure 4: Non-homogenous pressure trace from Mix 2. Observed non-idealities also present in OH* emission trace.

Since the mixtures studied in this work are being oxidized in air and undiluted, (all the molecules are diatomic or polyatomic) the resulting reflected shock wave experiences bifurcation, making it difficult to homogeneously ignite in the low-temperature region. An example of a non-ideal ignition trace is shown in Figure 4, which very clearly exhibits pressure and emissions signal rise before strong ignition (circled in red). Determination of the IDT cannot be well defined due to strong ignition occurring roughly 325 µs after pre-ignition onset. This phenomenon was seen in the low-temperature regions for all mixtures except for the rich conditions.

To prevent preignition, temperatures below 1070 K attempted to employ the constrained reaction volume (CRV) stage-filling approach refined by Hanson et al. at Stanford University [39-41] (displayed in Figure 5). In the CRV stage-filling technique, the fuel mixture is first added at a lower partial pressure. After that, non-reactive stage-filling gas is slowly introduced near the

diaphragm of the shock tube until the correct total $P_1$ is achieved, compressing the fuel mixture at the test section and preventing non-localized ignition. The stage-filling gas should closely match the specific heat ratio of the fuel mixture, as well as the average molecular weight of the mixture. This technique required characterization of the diffusivity between the two gases in order to prevent the stage-filling gas from diluting the fuel mixture. Preliminary tests were performed to determine if the process is viable using $CH_4/O_2/Ar$ mixtures stage-filled with argon (Ar). The total fill time was around 7 minutes.

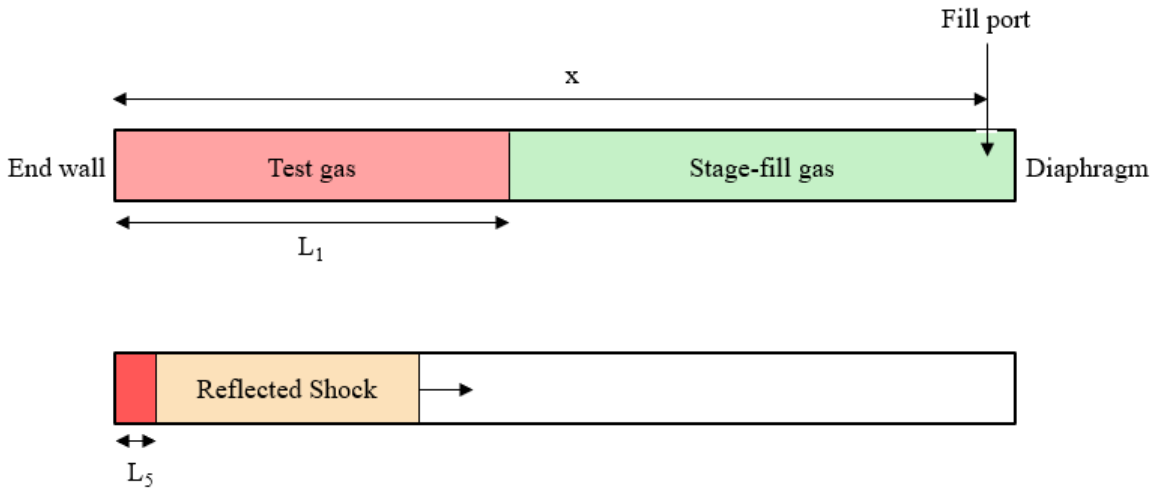


Figure 5: Illustration of the shock tube driven section CRV stage-filling. Subscript 1 refers to the state properties before the arrival of the incident shock wave. State 5 is the test conditions after the reflected shock wave.

Defined by Hanson et al., $L_1$, the initial length of the test gas before compression, is determined by using:

$$L_1 = L_5 \frac{\rho_5}{\rho_1} = L_5 \frac{P_5}{P_1} \frac{T_1}{T_5} \quad (3)$$

where the density ratio can be related to temperature and pressure relations using the ideal gas law. Substituting ideal shock equations for the pressure and temperature relations for a given Mach number:

$$\frac{P_5}{P_1} = \left\{\frac{2\gamma M_1^2 - (\gamma - 1)}{\gamma + 1}\right\}\left\{\frac{(3\gamma - 1)M_1^2 - 2(\gamma - 1)}{(\gamma - 1)M_1^2 + 2}\right\} \quad (4)$$

$$\frac{T_5}{T_1} = \frac{\{2(\gamma - 1)M_1^2 + (3 - \gamma)\}\{(3\gamma - 1)M_1^2 - 2(\gamma - 1)\}}{(\gamma + 1)^2 M_1^2} \quad (5)$$

and by specifying an optimal $L_5$ of approximately 4.5 cm, $L_1$ can be related to the mixture pressure using:

$$P_{1_{test\ gas}} = \frac{L_1 P_{1_{total}}}{x} \quad (6)$$

where *x* is the distance from the end wall to the fill location.

Diffusivity between the test gas and the stage-filled gas is inevitable but can be characterized with uncertainty if the fill-time is optimized to prevent turbulent mixing and gas-stratification, documented by Susa *et al*. [42]. Initial testing of 4% $CH_4$ / 8% $O_2$ / 88% Ar stage-filled with Ar (Figure 7) was attempted and showed a discrepancy in the post-reflected shock pressure when compared to the ideal shock equations' calculated pressure. A conventionally filled mixture with double the amount of Ar (2.13% $CH_4$ / 4.26% $O_2$ / 93.62% Ar, Figure 8) is shown except with the ideal shock equations' $P_5$ calculation performed as if there was no extra Ar addition, leading to a similar but exaggerated discrepancy shown in the stage-filled experiment (Figure 7).

The trace in Figure 6 is the same mixture as the stage-filled in Figure 7, except conventionally filled. PCB 5 is in good agreement with the ideal shock equations' calculations, which is normally seen in the facility experiments. A possible characterization to stage-filling that will be explored is to back-calculate $P_5$ to determine the amount of stage-filled gas that diluted the test mixture. From there, the uncertainty would be determined, however this is not considered to

be a trustworthy method and therefore the CRV stage-filling method was concluded not to be sufficient for high-pressure shocks and will not be employed for these experiments.

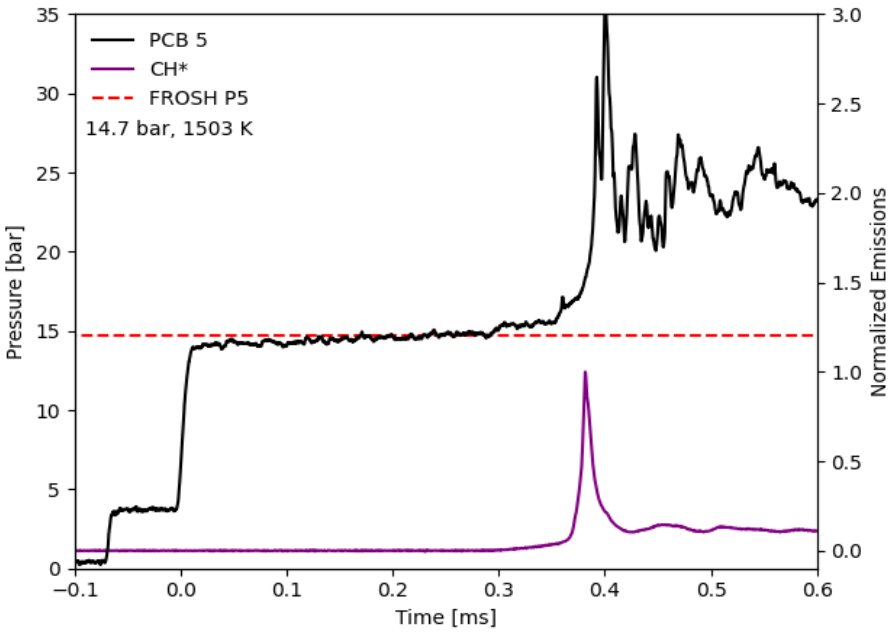


Figure 6: Conventionally filled pressure trace (black) showed to match theoretical calculated $P_5$ (red).

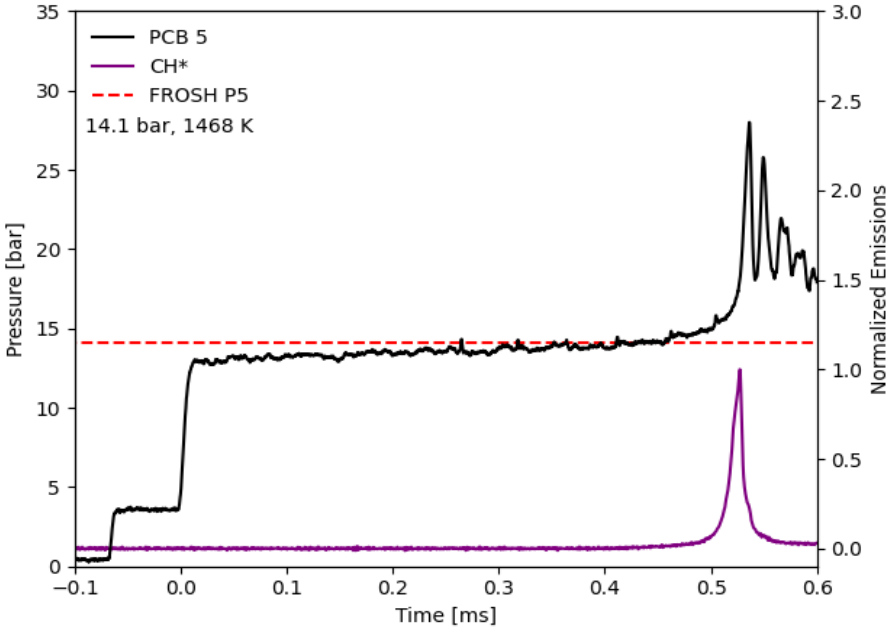


Figure 7: Stage-filled pressure trace (black) showed to deviate from theoretical calculated $P_5$ (red).

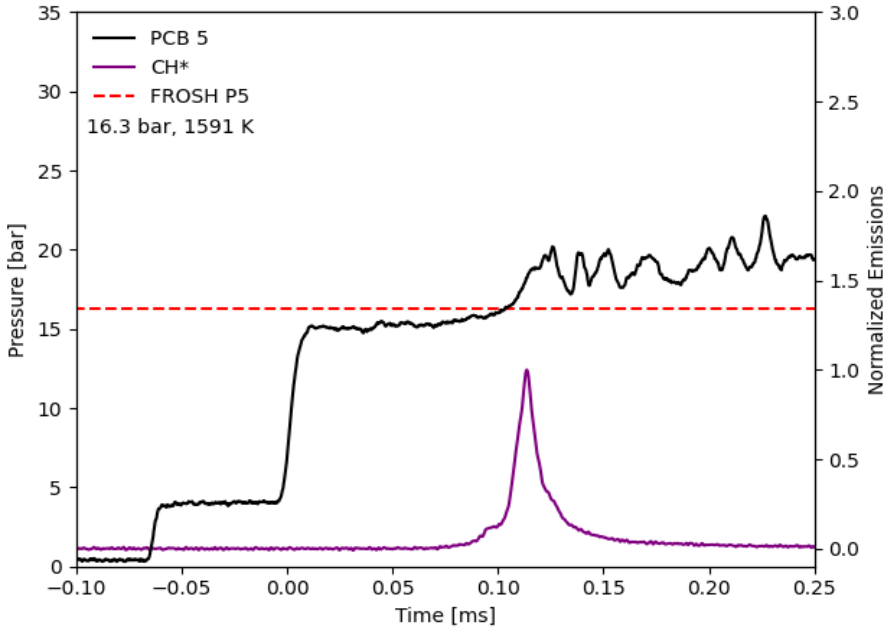


Figure 8: Conventionally filled pressure trace of a mixture containing double the amount of Ar (black) shown to deviate from theoretical calculated $P_5$ (red). FROSH $P_5$ was calculated without doubling Ar and the pressure trace deviates similar to the stage-filled mixture thus indicating that the stage-filled mixture was rather completely mixed.

# CHAPTER 4: EXPERIMENTAL RESULTS AND CHEMICAL KINETIC MODEL PERFORMANCE

## 4.1 IDT Analysis

The IDT measurements presented in Figures 9-11 were taken near 25 bar between a temperature range of 1000-1500 K. All collected points are listed in Table 2. Baseline mixtures of pure NG were taken to compare the addition of $H_2$ and $NH_3$ at each equivalence ratio. The NUIGMech 1.1 mechanism was used for simulations of each mixture at 25 bar (solid line) to show the logarithmic ignition trend across the entire temperature range. The experimental data are solid-filled points on the plot with a calculated 15% uncertainty, which is calculated from the uncertainty in the shock velocity and further explained by Urso *et al*. [22]. Hollow points represent the NUIGMech 1.1 simulated at the exact experimental pressure as the accompanying solid-filled experimental point, as some data points may be slightly above or below 25 bar. The mixtures are named based on their assigned "Mix" number in Table 1.

Table 2: Experimental IDT data for each mixture with pressure and temperature measurements

| Mix | P [bar] | T [K] | IDT [μs] |
|---|---|---|---|
| 1 | 22.1 | 1317 | 659 |
| | 23.2 | 1349 | 441 |
| | 25.2 | 1350 | 396 |
| | 24.3 | 1378 | 317 |
| | 24.3 | 1388 | 260 |
| | 26.2 | 1437 | 156 |
| 2 | 24.9 | 1091 | 993 |

| Mix | P [bar] | T [K] | IDT [µs] |
|---|---|---|---|
| | 24.7 | 1141 | 544 |
| | 25.2 | 1199 | 234 |
| | 26.1 | 1272 | 88 |
| | 27.1 | 1292 | 68 |
| 3 | 26.1 | 1271 | 864 |
| | 25.1 | 1292 | 786 |
| | 22.6 | 1367 | 418 |
| | 26.0 | 1427 | 216 |
| | 25.4 | 1492 | 101 |
| | 25.8 | 1522 | 74 |
| 4 | 22.9 | 1280 | 751 |
| | 23.5 | 1304 | 641 |
| | 24.8 | 1341 | 383 |
| | 26.1 | 1404 | 223 |
| | 23.7 | 1435 | 138 |
| 5 | 24.2 | 1118 | 653 |
| | 25.7 | 1138 | 530 |
| | 26.2 | 1174 | 367 |
| | 25.6 | 1186 | 332 |
| | 26.9 | 1216 | 227 |

| Mix | P [bar] | T [K] | IDT [µs] |
|---|---|---|---|
| | 26.7 | 1246 | 139 |
| | 24.4 | 1268 | 122 |
| 6 | 22.7 | 1209 | 1586 |
| | 23.9 | 1230 | 1353 |
| | 24.8 | 1263 | 1043 |
| | 23.5 | 1307 | 699 |
| | 23.8 | 1315 | 671 |
| | 24.3 | 1323 | 600 |
| | 24.9 | 1364 | 373 |
| | 25.4 | 1403 | 257 |
| | 24.8 | 1479 | 150 |
| 7 | 27.2 | 1200 | 1401 |
| | 26.7 | 1232 | 1082 |
| | 27.2 | 1248 | 964 |
| | 25.5 | 1261 | 1075 |
| | 25.9 | 1263 | 908 |
| | 25.5 | 1288 | 768 |
| | 26.0 | 1317 | 598 |
| | 27.1 | 1395 | 210 |
| 8 | 24.3 | 1027 | 1743 |

| Mix | P [bar] | T [K] | IDT [μs] |
|---|---|---|---|
| | 26.0 | 1032 | 1593 |
| | 25.5 | 1040 | 1444 |
| | 24.7 | 1050 | 1296 |
| | 25.9 | 1076 | 944 |
| | 26.3 | 1078 | 936 |
| | 26.1 | 1081 | 936 |
| | 25.3 | 1101 | 732 |
| | 25.6 | 1184 | 256 |
| | 24.5 | 1195 | 206 |
| | 25.0 | 1211 | 174 |
| 9 | 25.9 | 1217 | 1437 |
| | 25.4 | 1221 | 1422 |
| | 25.7 | 1259 | 951 |
| | 25.7 | 1263 | 949 |
| | 26.9 | 1319 | 551 |
| | 26.2 | 1325 | 586 |
| | 24.9 | 1329 | 590 |
| | 26.1 | 1405 | 277 |

Figures 9-11 are fuel-independent IDT plots of baseline NG, NG/$H_2$, and NG/$NH_3$, respectively, comparing the changing equivalence ratio effects on ignition. Stoichiometric

conditions are black circles, rich conditions are red squares, and lean conditions are blue triangles, which are consistent for this set of plots.

Figure 9 shows the IDTs for pure NG mixtures at different equivalence ratios. In general, experimental IDTs tend to decrease with increasing temperature. At 1437 K, the IDT was found to be 156 μs, though a decrease in ~120 K increases the IDT to ~650 μs at 1317 K and Φ=1.0. For Φ=0.5, IDT is found to be 138 μs at 1435 K, while at 1304 K, it is 640 μs. Previous studies [43] indicate that dilute hydrocarbon mixtures ignite faster at fuel-lean conditions (Φ=0.5) while slowing down ignition at fuel-rich conditions (Φ=2.0). However, in undiluted conditions, only a negligible difference is observed in IDTs for lean and stoichiometric conditions. This is primarily due to the higher concentration of fuel in stoichiometric cases than in lean cases. At high temperatures (~ 1400 K), the fuel-rich mixture (Φ=2.0) ignites faster than its Φ=1.0 and Φ=0.5 counterparts and shows similar IDTs (598 μs at 1317 K) at lower temperatures as evident from Figure 9. Similar observations are made with NG/$H_2$ mixtures (Figure 10), where the lean case shows the longest IDTs followed by stoichiometric and rich cases. Negative temperature coefficient (NTC) behavior was not seen in any case, unlike the results found by De Vries and Petersen [17] however, their study was in the lower temperature region where NTC is more commonly observed with $CH_4$ [44]. As mentioned in Chapter 3.2, concentrations of higher-order hydrocarbons were exceptionally low in the NG mixture and therefore the pure NG mix was expected to behave close to pure methane. This conclusion for NTC behavior is similarly drawn since NTC of large alkanes occurs near the same temperature region of $CH_4$ [44].

Model agreement is excellent for stoichiometric conditions (apart from Mix 1), supporting that undiluted mixtures do not have a significant effect on ignition chemistry. De Vries and

Petersen [17] similarly showed that ignition with methane does not change if an Ar bath gas is replaced with $N_2$, however, NO pathways for air-breathing engines using $NH_3$ can be affected if excess $N_2$ is present in the combustion, and ultimately affect emissions and ignition. For these cases, the $N_2$ chemistry from the NO sub-mechanism predicts very accurate IDTs in all mixture conditions. Baseline NG ignition did not change with changing equivalence ratios (Figure 9), whereas NG/$H_2$ mixtures auto-ignited faster in rich conditions and slowed in the lean conditions, which the model accurately predicts (Figure 10). NG/$NH_3$ experimental data shows that changing the equivalence ratio did not affect ignition, similar to pure NG. However, the model predicted lean conditions to be quicker and rich conditions to ignite slower (Figure 11).

When increasing or decreasing the equivalence ratio, pure NG IDTs became faster than the model predictions at all temperatures while NG/$H_2$ were also slightly faster than the model at lower points in the temperature range. Additionally, NG/$H_2$ ignition shows to trend linearly with changing temperature for stoichiometric and rich cases but non-linearly for lean conditions, which the model fails to capture.

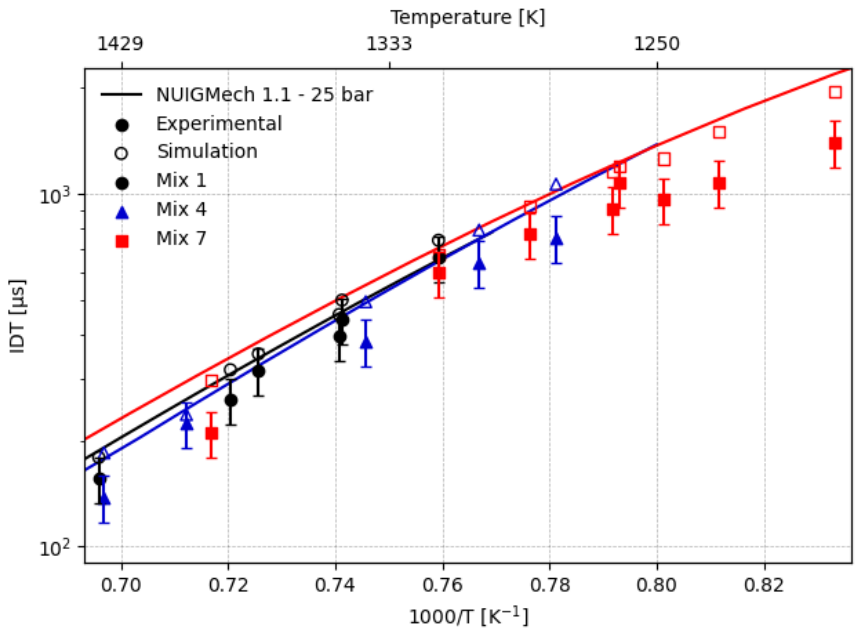


Figure 9: Experimental baseline NG IDTs compared to chemical kinetic model. (Mix 1 is at Φ=1.0, Mix 4 is at Φ=0.5, and Mix 7 is at Φ=2.0).

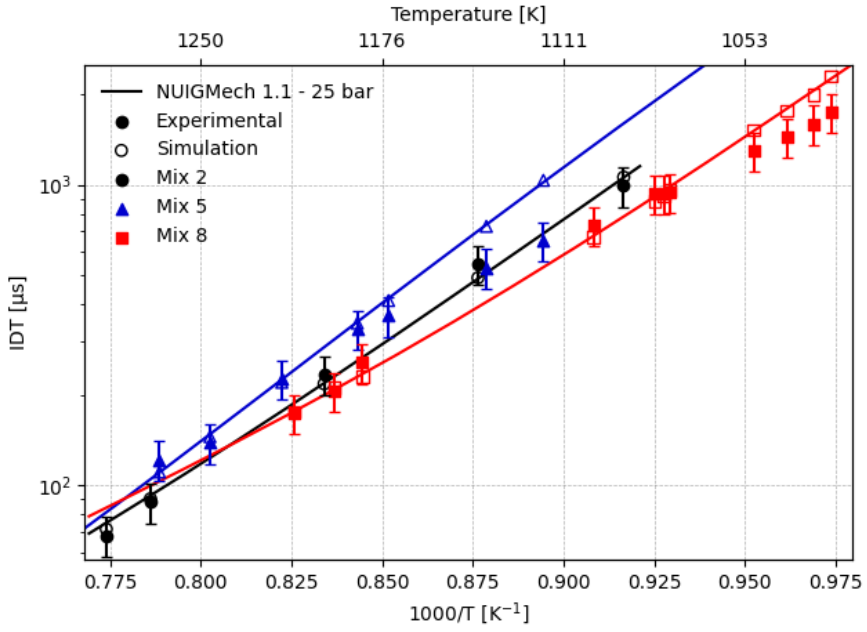


Figure 10: Experimental NG/$H_2$ IDTs compared to chemical kinetic model. (Mix 2 is at Φ=1.0, Mix 5 is at Φ=0.5, and Mix 8 is at Φ=2.0).

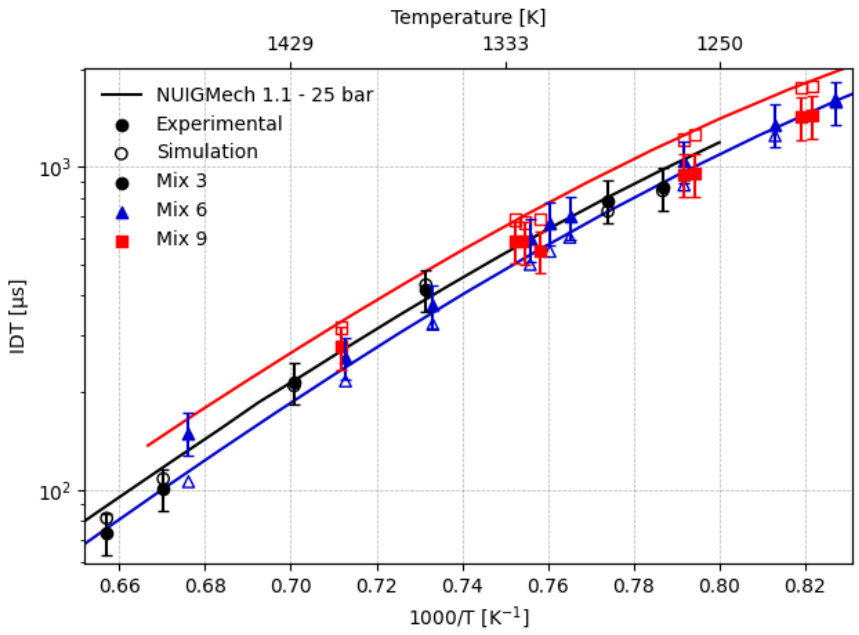


Figure 11: Experimental NG/$NH_3$ IDTs compared to chemical kinetic model. (Mix 3 is at Φ=1.0, Mix 6 is at Φ=0.5, and Mix 9 is at Φ=2.0).

## 4.2 Effect of Hydrogen and Ammonia Addition

For this section, baseline NG mixtures are black circles, mixtures with $NH_3$ addition are red squares, and $H_2$-containing mixtures are blue triangles. Figure 12 shows stoichiometric conditions, Figure 13 compares lean conditions, and Figure 14 compares rich conditions.

Similar to the analysis made by Baker *et al*. [20], $H_2$ addition very significantly increases the reactivity of the mixture, thus experiencing much quicker IDTs. Hydrogen addition decreases the IDT by approximately 90% for stoichiometric conditions (Figure 12), 86% for lean conditions (Figure 13), and 89% for rich conditions (Figure 14). Conversely, $NH_3$ addition shows little effect on the ignition when compared to the baseline. These observations can be attributed to dominating $H_2$ chemistry for NG/$H_2$ mixtures whereas NG/$NH_3$ mixtures are dominated by hydrocarbon chemistry. Further analysis of the chemistry between these reactions is found in Chapter 4.4. Baker

*et al*. [20] also noted that $NH_3$ greatly decreased the reactivity of the mixture in their study when compared to baseline NG. However, the NG mixture used contained larger amounts of higher order hydrocarbons, whereas this study only contains ppm quantities (<770 ppm $C_3H_8$ and <51 ppm $C_4H_{10}$), hence supporting that the higher order alkanes play little role in the ignition behavior when in small quantities. Baker *et al*. [20] similarly suggested that the larger hydrocarbons initially formed OH radicals faster than the rest of the reactants.

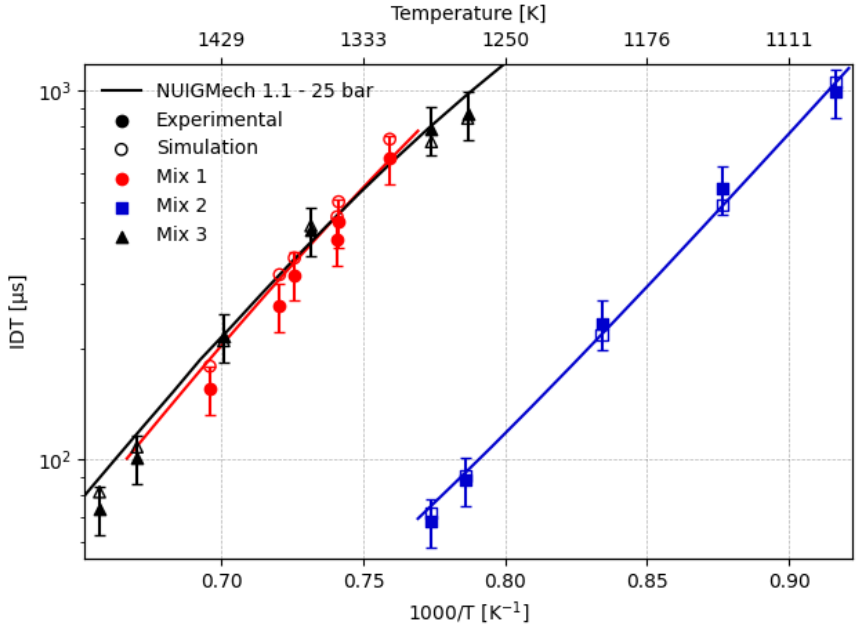


Figure 12: Experimental stoichiometric (Φ=1.0) IDTs compared to chemical kinetic model. (Mix 1 is baseline NG, Mix 2 is NG/$H_2$, and Mix 3 is NG/$NH_3$).

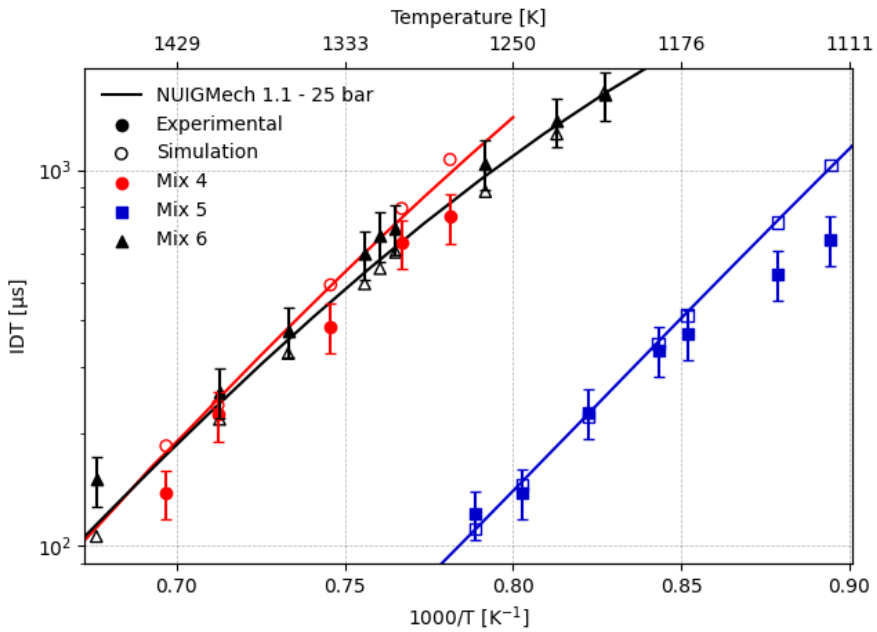


Figure 13: Experimental lean (Φ=0.5) IDTs compared to chemical kinetic model. (Mix 4 is baseline NG, Mix 5 is NG/$H_2$, and Mix 6 is NG/$NH_3$).

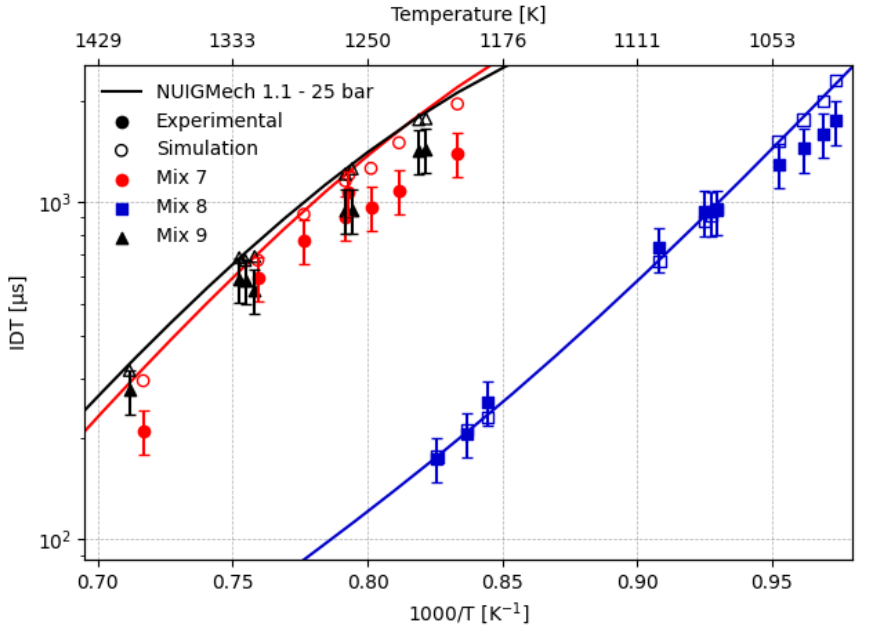


Figure 14: Experimental rich (Φ=2.0) IDTs compared to chemical kinetic model. (Mix 7 is baseline NG, Mix 8 is NG/$H_2$, and Mix 9 is NG/$NH_3$).

## 4.3 Sensitivity Analysis

Sensitivity analyses between mixtures are shown in Figures 15-18 to find shared reactions that are most prominent to ignition. As noted in Chapter 3.4, each sensitivity analysis was performed using OH formation rather than a fuel decomposition due to the blending from multiple fuels. Although this does not affect the sensitivity analysis, it does change the perspective of the sensitivity coefficients. Therefore, positive sensitivity coefficients are indicative of ignition-promoting reactions, while negative sensitivity coefficients are ignition-inhibiting reactions.

Lower temperature pure NG ignition for stoichiometric conditions is mainly dominated by the $CH_3$ reactions,

$$CH_3 + O_2 = CH_2O + OH \quad \text{(R114)}$$

$$CH_3 + HO_2 = CH_3O + OH \quad \text{(R122)}$$

as shown in Figure 16. The breakdown of the C-H bond also frees an H atom and promotes the chain-branching reaction,

$$O_2 + H = O + OH \quad \text{(R10)}$$

which is an elementary reaction in the hydrocarbon ignition process. (R10) is also very sensitive to NG/$H_2$ ignition because of the H-H bond separation in $H_2$. This reaction is then expedited due to two readily available H atoms rather than the one from C-H. The early onset of (R10) consumes available $O_2$ and inhibits methyl oxidation, leading to hydrocarbon pyrolysis rather than oxidation. With no free $O_2$ molecules leftover H atoms bond together, leaving large amounts of $H_2$ in the products of the combustion. This pattern was common for all NG/$H_2$ mixtures, especially for fuel-rich conditions.

Unlike the $H_2$ addition, $NH_3$ does not heavily affect the sensitive reactions to OH. Many of the commonly shared reactions of pure NG and NG/$NH_3$ in Figure 18 have similar effects on ignition, indicating that hydrocarbon chemistry is dominant. (R10), (R114), and (R122) are still the most prominent reactions however mainly from C-H breakdown in these cases. This similarly causes pyrolyzation of nitrogen chemistry and creates free H atoms from N-H separation, thus still leaving ample amounts of $H_2$ in the combustion products.

As discussed earlier in Chapter 4.1, NG/$NH_3$ chemistry is affected by the presence of air ($N_2$) in replacement for Ar. During the combustion, high-temperature thermal NO begins through the chain reaction,

$$N + O_2 = NO + O \qquad \text{(R10467)}$$

through which,

$$NO + HO_2 = NO_2 + OH \qquad \text{(R10517)}$$

is initiated and promotes OH radical production. Figure 17 shows (R10517) to be an ignition-promoting reaction for stoichiometric mixtures of NG/$NH_3$. Although this reaction sequence is also driven by fuel NO from ammonia, energy is first required to break N-H bonds to get free NH molecules whereas an N-N bond separation readily frees two N atoms from $N_2$ in air. In the case of these mixtures, NH molecules from pyrolyzed $NH_3$ and separated N-N bonds are both contributing to NO in (R10467).

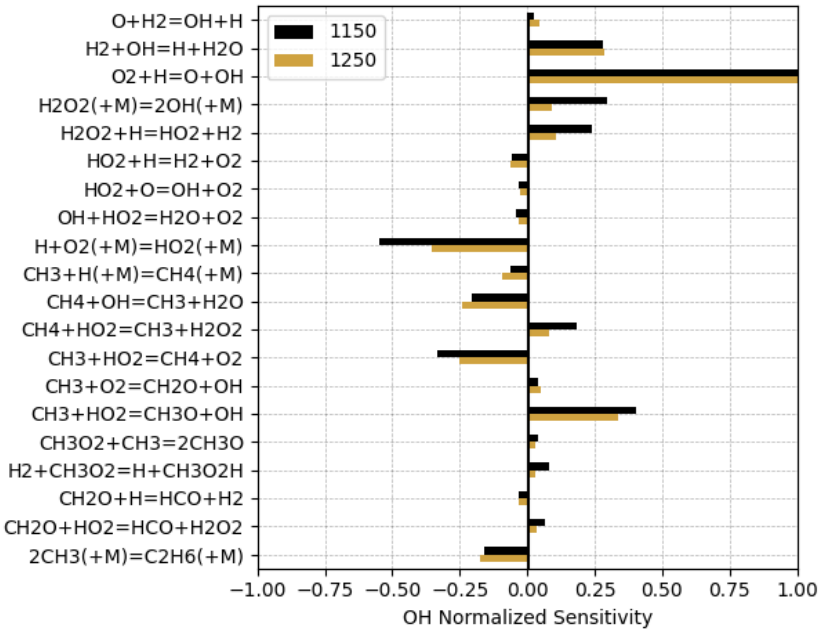


Figure 15: Stoichiometric NG/$H_2$ sensitivity analysis at 1150 K and 1250 K.

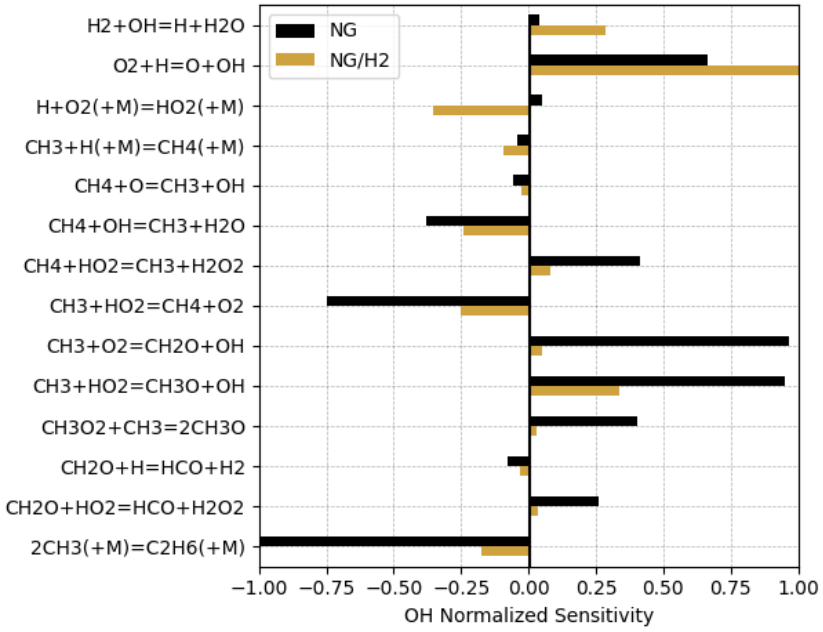


Figure 16: Stoichiometric NG/$H_2$ sensitivity analysis at 1250 K compared to baseline NG.

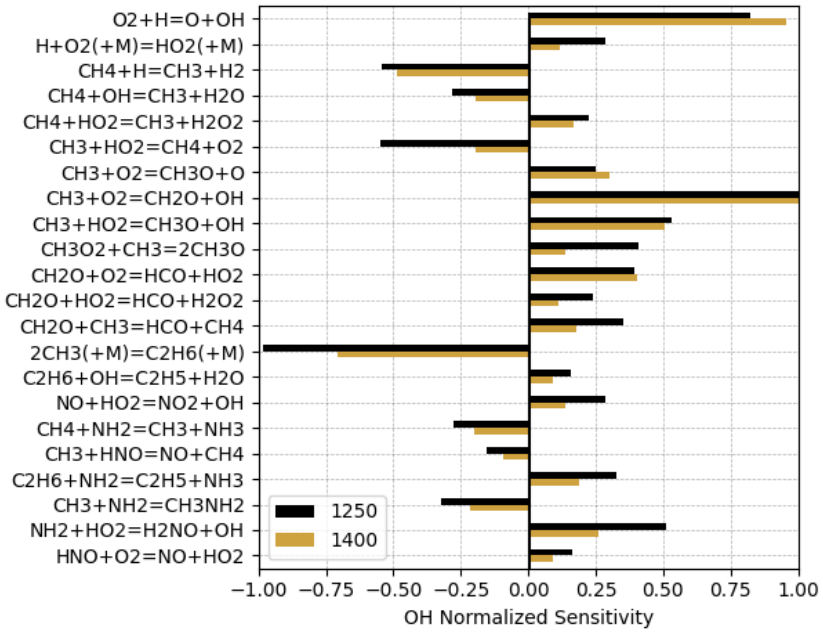


Figure 17: Stoichiometric NG/$NH_3$ sensitivity analysis at 1250 K and 1400 K.

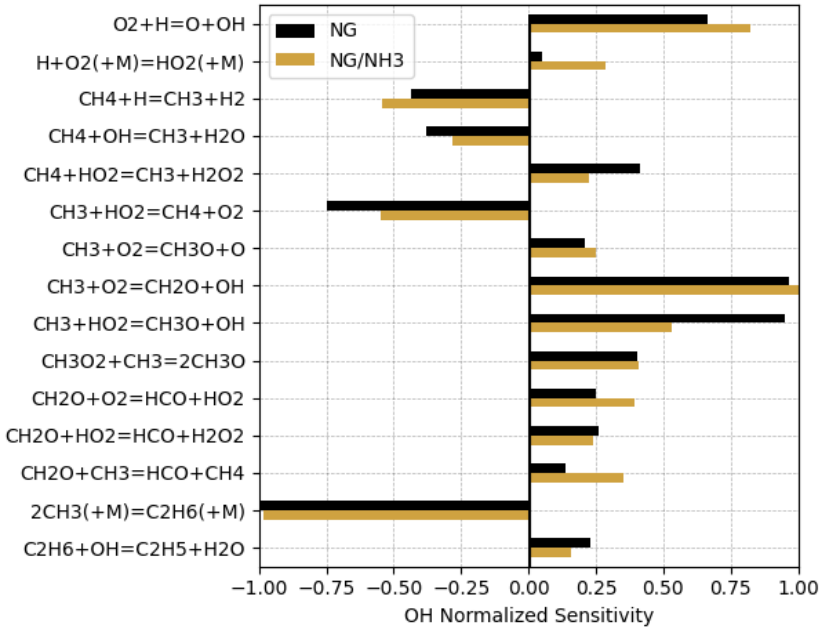


Figure 18: Stoichiometric NG/$NH_3$ sensitivity analysis at 1250 K compared to baseline NG.

Further sensitivity analyses for pure NG model improvement are shown in Figures 19 and 20. As noted earlier, experimental data points at each equivalence ratio are moderately faster than the NUIGMech 1.1 predictions. A change in the rate coefficient (*k*) for a reaction that would linearly shift the model predictions toward the experimental data may match better. The reaction,

$CH_3 + O_2 = CH_3O + O$ (R118)

is shared for all baseline NG mixtures at high and low temperatures in the sensitivity analyses and would also equally shift each prediction closer towards the data since the normalized sensitivity coefficients are similar in magnitude at both 1250 and 1400 K. Upon investigation of (R118), the listed uncertainty in k is more than ±30% from work done by Srinivasan *et al*. [45], giving a large range of adjustability. (R118) is also only commonly shared amongst the pure NG mixture, which would not significantly affect the agreement of the model with mixtures containing $H_2$ and $NH_3$ addition. A brief investigation into solely decreasing the A-factor of (R118) by 30% decreased the IDTs by as much as 8%, depending on the mixture and temperature. More experimental data at alternative pressures and temperatures from proceeding studies and thorough chemical analyses are required to compare the model performance before any modifications can be made to the chemical kinetic mechanism.

Alternatively, decreasing *k* of the inhibiting reaction,

$2CH_3 (+M) = C_2H_6 (+M)$ (R227)

may also bring the model closer in agreement and has been calculated with a ±20% in the work of Blitz *et al*. [46]. However, this reaction is not advised to be modified because it is commonly shared in the NG/$H_2$ and NG/$NH_3$ mixtures, which are already mostly in agreement with the model.

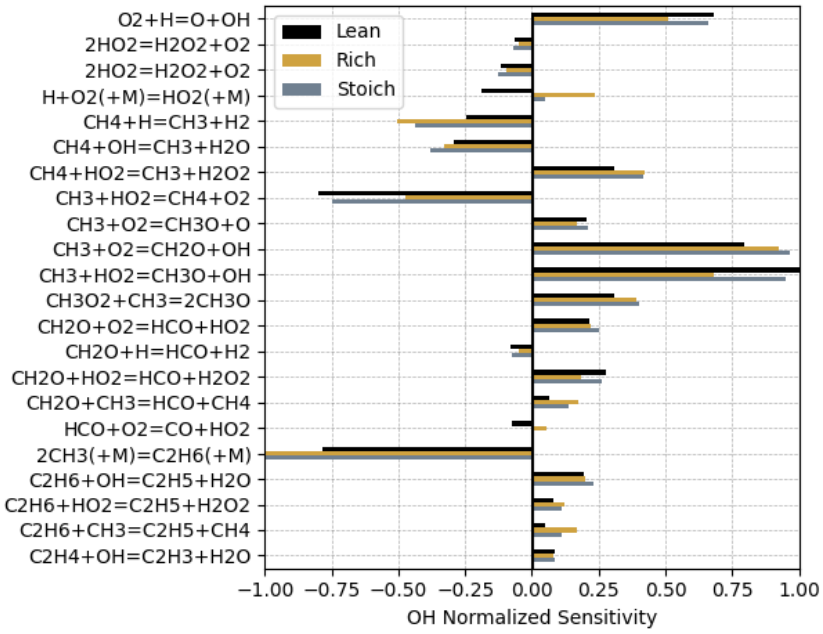


Figure 19: Pure NG sensitivity analysis at 1250 K.

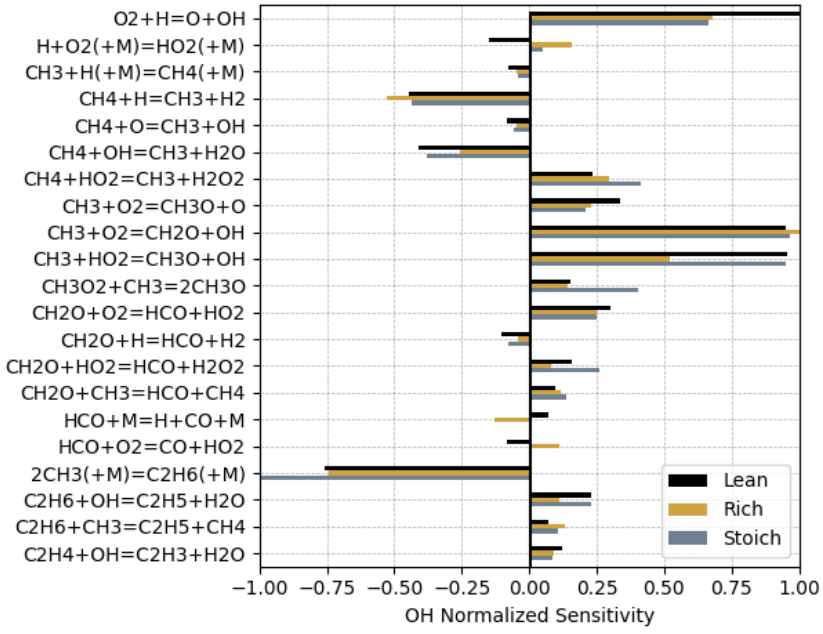


Figure 20: Pure NG sensitivity analysis at 1400 K.

# CHAPTER 5: SUMMARY

In this work, hydrogen and ammonia addition to natural gas mixtures ignition was probed under gas turbine operating conditions. Equal amounts of hydrogen and ammonia were added to undiluted, pre-mixed mixtures of natural gas/air and combusted at the conditions relevant to current gas turbine operating conditions (1000-1500 K, 25 bar). The ignition delay times are reported here within and compared to the NUIGMech 1.1 for undiluted, high-fuel validation. Similar studies of undiluted NG mixtures have yet to be performed, but comparisons are made to fundamental work by De Vries and Petersen [17] as well as Baker *et al*. [20], who have performed relevant work. The work performed in this study is an initial step towards lowering carbon emissions for current NG turbines. The main conclusions of the study are as follows:

1. The NUIGMech 1.1 model shows good agreement for stoichiometric conditions but deviates during lean and rich conditions. Previously, undiluted chemistry effects on ignition at higher pressures were not explored but are now validated for chemical kinetic modeling. Pure NG measurements were moderately faster than the predictions, making a further analysis into relating reaction coefficients a necessary step to improve the model.

2. 50% $H_2$ fuel fraction greatly decreases IDT while $NH_3$ shows to have no effect at the tested conditions. An analysis of the reactions in the ignition process shows dominating hydrogen chemistry for mixtures containing $H_2$ and dominating hydrocarbon chemistry for mixtures containing $NH_3$. While validation of emissions formation of CO and $NO_x$ is still imperative, from an ignition standpoint, $NH_3$ addition looks like a promising and favorable modification to current NG turbines without needing a major infrastructure change.

3. Sensitivity analyses show large differences in the sensitive coefficient between stoichiometric pure NG and NG/$H_2$. Stoichiometric NG/$NH_3$ share very similar sensitivity coefficients with pure NG, further supporting that hydrocarbon chemistry dominates ignition rather than inhibiting nitrogen chemistry. The reaction $CH_3 + O_2 = CH_3O + O$ is suggested as a modifiable parameter to improve the model performance of pure NG, although not necessary for predicting $H_2$ and $NH_3$ ignition.

# LIST OF REFERENCES


[1] H. A. Haugen, N. H. Eldrup, A. M. Fatnes, and E. Leren, "Commercial capture and transport of CO2 from production of ammonia," *Energy Procedia*, vol. 114, pp. 6133-6140, 2017.

[2] O. Tuncer, S. Acharya, and J. Uhm, "Dynamics, NOx and flashback characteristics of confined premixed hydrogen-enriched methane flames," *International Journal of hydrogen energy*, vol. 34, no. 1, pp. 496-506, 2009.

[3] N. Syred, M. Abdulsada, A. Griffiths, T. O'Doherty, and P. Bowen, "The effect of hydrogen containing fuel blends upon flashback in swirl burners," *Applied Energy*, vol. 89, no. 1, pp. 106-110, 2012.

[4] A. A. Khateeb, T. F. Guiberti, X. Zhu, M. Younes, A. Jamal, and W. L. Roberts, "Stability limits and exhaust NO performances of ammonia-methane-air swirl flames," *Experimental Thermal and Fluid Science*, vol. 114, p. 110058, 2020.

[5] D. Pratt, "Performance of ammonia-fired gas-turbine combustors," California Univ Berkeley Thermal Systems Div, 1967.

[6] H. Tian *et al.*, "A comprehensive quantification of global nitrous oxide sources and sinks," *Nature*, vol. 586, no. 7828, pp. 248-256, 2020.

[7] L. Alves *et al.*, "A comprehensive review of NOx and N2O mitigation from industrial streams," *Renewable and Sustainable Energy Reviews*, p. 111916, 2021.

[8] A. Jain, S. Agarwal, and T. Ichikawa, "5 Ammonia: a promising candidate for hydrogen economy," *Hydrogen Storage for Sustainability*, p. 225, 2021.

[9] M. Aziz, A. T. Wijayanta, and A. B. D. Nandiyanto, "Ammonia as effective hydrogen storage: A review on production, storage and utilization," *Energies*, vol. 13, no. 12, p. 3062, 2020.

[10] C. Zamfirescu and I. Dincer, "Using ammonia as a sustainable fuel," *Journal of Power Sources*, vol. 185, no. 1, pp. 459-465, 2008.

[11] C. F. Ramos, R. C. Rocha, P. M. Oliveira, M. Costa, and X.-S. Bai, "Experimental and kinetic modelling investigation on NO, CO and NH3 emissions from NH3/CH4/air premixed flames," *Fuel*, vol. 254, p. 115693, 2019.

[12] N. Donohoe *et al.*, "Ignition delay times, laminar flame speeds, and mechanism validation for natural gas/hydrogen blends at elevated pressures," *Combustion and Flame*, vol. 161, no. 6, pp. 1432-1443, 2014.

[13] W. S. Chai, Y. Bao, P. Jin, G. Tang, and L. Zhou, "A review on ammonia, ammonia-hydrogen and ammonia-methane fuels," *Renewable and Sustainable Energy Reviews*, vol. 147, p. 111254, 2021.

[14] S. Gersen, N. Anikin, A. Mokhov, and H. Levinsky, "Ignition properties of methane/hydrogen mixtures in a rapid compression machine," *International Journal of Hydrogen Energy*, vol. 33, no. 7, pp. 1957-1964, 2008.

[15] J. Herzler and C. Naumann, "Shock-tube study of the ignition of methane/ethane/hydrogen mixtures with hydrogen contents from 0% to 100% at different pressures," *Proceedings of the combustion institute*, vol. 32, no. 1, pp. 213-220, 2009.

[16] J. Huang, W. Bushe, P. Hill, and S. Munshi, "Experimental and kinetic study of shock initiated ignition in homogeneous methane–hydrogen–air mixtures at engine-relevant

conditions," *International Journal of Chemical Kinetics,* vol. 38, no. 4, pp. 221-233, 2006.

[17] J. De Vries and E. Petersen, "Autoignition of methane-based fuel blends under gas turbine conditions," *Proceedings of the combustion institute,* vol. 31, no. 2, pp. 3163-3171, 2007.

[18] A. R. Laich *et al.,* "Ignition Behavior of Oxy-Methane With High Fuel Loading and CO2 Dilution in a Shock Tube," in *Turbo Expo: Power for Land, Sea, and Air*, 2020, vol. 84126: American Society of Mechanical Engineers, p. V04AT04A012.

[19] B. Shu, X. He, C. Ramos, R. Fernandes, and M. Costa, "Experimental and modeling study on the auto-ignition properties of ammonia/methane mixtures at elevated pressures," *Proceedings of the Combustion Institute,* vol. 38, no. 1, pp. 261-268, 2021.

[20] J. Baker *et al.*, "Experimental Ignition Delay Time Measurements and Chemical Kinetics Modeling Of Hydrogen/Ammonia/Natural Gas Fuels," *Journal of Engineering for Gas Turbines and Power,* 2022.

[21] R. Li, A. A. Konnov, G. He, F. Qin, and D. Zhang, "Chemical mechanism development and reduction for combustion of NH3/H2/CH4 mixtures," *Fuel,* vol. 257, p. 116059, 2019.

[22] J. J. Urso *et al.*, "Characterization of a new ultra-high pressure shock tube facility for combustion and propulsion studies," *Review of Scientific Instruments,* vol. 93, no. 6, p. 063905, 2022.

[23] *PyRGFROSH: A frozen shock solver for ideal and real gas equations of state*. (2022). [Online]. Available: https://vasulab.github.io/PyRGFROSH

[24] G. Bourque *et al.*, "Effect of Higher-Order Hydrocarbons on Methane-Based Fuel Chemistry at Gas Turbine Pressures," in *Turbo Expo: Power for Land, Sea, and Air*, 2007, vol. 47918, pp. 781-788.

[25] M. Pierro, A. Laich, J. J. Urso, C. Kinney, S. Vasu, and M. A. Albright, "Ignition delay times of methane fuels at thrust chamber conditions in an ultra-high-pressure shock tube," in *AIAA SCITECH 2022 Forum*, 2022, p. 1254.

[26] O. Mathieu and E. L. Petersen, "Experimental and modeling study on the high-temperature oxidation of Ammonia and related NOx chemistry," *Combustion and flame*, vol. 162, no. 3, pp. 554-570, 2015.

[27] M. Pochet, V. Dias, B. Moreau, F. Foucher, H. Jeanmart, and F. Contino, "Experimental and numerical study, under LTC conditions, of ammonia ignition delay with and without hydrogen addition," *Proceedings of the Combustion Institute*, vol. 37, no. 1, pp. 621-629, 2019.

[28] E. Petersen and R. Hanson, "Measurement of reflected-shock bifurcation over a wide range of gas composition and pressure," *Shock Waves*, vol. 15, no. 5, pp. 333-340, 2006.

[29] E. L. Petersen, "Interpreting endwall and sidewall measurements in shock-tube ignition studies," *Combustion science and technology*, vol. 181, no. 9, pp. 1123-1144, 2009.

[30] B. Shu *et al.*, "A shock tube and modeling study on the autoignition properties of ammonia at intermediate temperatures," *Proceedings of the Combustion Institute*, vol. 37, no. 1, pp. 205-211, 2019.

[31] Y. Wu *et al.*, "Understanding the antagonistic effect of methanol as a component in surrogate fuel models: A case study of methanol/n-heptane mixtures," *Combustion and Flame,* vol. 226, pp. 229-242, 2021.

[32] P. Glarborg, J. A. Miller, B. Ruscic, and S. J. Klippenstein, "Modeling nitrogen chemistry in combustion," *Progress in Energy and Combustion Science,* vol. 67, pp. 31-68, 2018.

[33] *Cantera: An Object-oriented Software Toolkit for Chemical Kinetics, Thermodynamics, and Transport Processes*. (2022). https://www.cantera.org.

[34] *ANSYS Chemkin*. ANSYS, Inc, Release 22.0 R2.

[35] S. Neupane *et al.*, "Shock tube/laser absorption and kinetic modeling study of triethyl phosphate combustion," *The Journal of Physical Chemistry A,* vol. 122, no. 15, pp. 3829-3836, 2018.

[36] H. Mark, "The interaction of a reflected shock wave with the boundary layer in a shock tube," 1958.

[37] R. N. Hollyer Jr, "a Study of Attenuation in the Shock Tube," *Ph. D. Thesis*, 1954.

[38] J. K. Hiroki Yamashita, Yuta Sugiyama, Akiko Matsuo, "Visualization study of ignition modes behind bifurcated-reflected shock waves," *Combustion and Flame,* vol. 159, no. 9, pp. 2954-2966, 2012, doi: https://doi.org/10.1016/j.combustflame.2012.05.009.

[39] R. K. Hanson, G. A. Pang, S. Chakraborty, W. Ren, S. Wang, and D. F. Davidson, "Constrained reaction volume approach for studying chemical kinetics behind reflected shock waves," *Combustion and flame,* vol. 160, no. 9, pp. 1550-1558, 2013.

[40] Y. Zhu, D. F. Davidson, and R. K. Hanson, "1-Butanol ignition delay times at low temperatures: An application of the constrained-reaction-volume strategy," *Combustion and flame,* vol. 161, no. 3, pp. 634-643, 2014.

[41] M. F. Campbell, A. M. Tulgestke, D. F. Davidson, and R. K. Hanson, "A second-generation constrained reaction volume shock tube," *Review of Scientific Instruments,* vol. 85, no. 5, p. 055108, 2014.

[42] A. Susa, D. Davidson, and R. Hanson, "Gravity-current-induced test gas stratification and its prevention in constrained reaction volume shock-tube experiments," *Shock Waves,* vol. 29, no. 7, pp. 969-984, 2019.

[43] C. Zhang, B. Li, F. Rao, P. Li, and X. Li, "A shock tube study of the autoignition characteristics of RP-3 jet fuel," *Proceedings of the Combustion Institute,* vol. 35, no. 3, pp. 3151-3158, 2015.

[44] D. Kaczmarek, S. Shaqiri, B. Atakan, and T. Kasper, "The influence of pressure and equivalence ratio on the NTC behavior of methane," *Proceedings of the Combustion Institute,* vol. 38, no. 1, pp. 233-241, 2021.

[45] N. Srinivasan, M.-C. Su, J. Sutherland, and J. Michael, "Reflected shock tube studies of high-temperature rate constants for CH3+ O2, H2CO+ O2, and OH+ O2," *The Journal of Physical Chemistry A,* vol. 109, no. 35, pp. 7902-7914, 2005.

[46] M. A. Blitz *et al.*, "Reanalysis of rate data for the reaction CH3+ CH3→ C2H6 using revised cross sections and a linearized second-order master equation," *The Journal of Physical Chemistry A,* vol. 119, no. 28, pp. 7668-7682, 2015.